ELSEVIER

Thermochimica Acta 332 (1999) 1–19

thermochimica acta

The use of experimental thermodynamic data in the phase equilibria verification

Zbigniew Moser[a,*], Krzysztof Fitzner[b]

[a]*Institute of Metallurgy and Materials Science, Polish Academy of Sciences, 25 Reymonta st., 30-059 Kraków, Poland*
[b]*Faculty of Non-Ferrous Metals, Division of Physical Chemistry and Electrochemistry, Academy of Mining and Metallurgy, 30 Al. Mickiewicza, 30-059 Kraków, Poland*

Received 16 July 1998; received in revised form 10 March 1999; accepted 11 March 1999

Abstract

This presentation summarises shortly the following experimental techniques: emf with liquid and solid electrolytes, vapour pressure measurements and calorimetric studies in application to metallic alloys. It is shown that usually one experimental technique is not sufficient for a reliable separation of the Gibbs energy into appropriate entropy and enthalpy contributions, which is necessary if one seeks the correlation between thermodynamic properties and phase equilibria. Critical assessment of the data available from different sources must be performed to get the proper thermodynamic information. Several specific examples will be analysed for systems with the miscibility gap and with intermetallic compounds to demonstrate this point of view. In some cases the correlation will be extended on the physical properties of alloys as well as the structure.

There are, however, some cases for which new experimental data are still needed to clarify the phase equilibria. Two examples from the field of calorimetry and emf measurements will be discussed to show how thermodynamic information must be coupled with the phase diagram investigations to obtain proper results:

- *Calorimetric measurements*. Results obtained in Cu–As and Ge–As systems will be shown and compared with existing binary phase diagrams. New data on the enthalpy of formation of solid and liquid Ge–As alloys let the description of the thermodynamic representation of the binary system be improved and express some doubts about the shape of the Ge–As phase diagram.
- *emf studies*. Results of electrochemical measurements with solid CaF_2 electrolytes on Yb–Ba–Cu–O systems are analysed. This example indicates how emf results can be misinterpreted if simultaneous investigations of phase equilibria are not conducted.

Keywords: emf; Vapour pressure; Calorimetric measurements; Phase equilibria; Phase diagram calculations

1. Introduction

The knowledge of detailed phase equilibria in high temperature systems is of primary importance in designing new materials used in modern technologies. Therefore, numerous research activities are still under way to supply new data as well as to improve existing information. It seems to be a proper idea to have a quick look at the route which scientific community had to follow before the present state of art was reached.

The interesting observation is to indicate that for long time thermodynamic studies and those dealing with phase equilibria were conducted separately. Sys-

*Corresponding author. Tel.: 48-12-3743200; fax: 48-12-6372192; e-mail: nmmoser@imim-pan.krakow.pl

0040-6031/99/$ – see front matter
PII: S0040-6031(99)00061-1

tematic accumulation of the thermodynamic properties of inorganic substances started probably with the work of Kelley [1] in 1935 with his ''Contribution to the Data on Thermochemical Metallurgy'' issued by the Bureau of Mines. A couple of years later, in 1943 during the Second World War, the book: ''Thermochemie der Legierungen'' by Weibke and Kubaschewski [2] appeared, which contained the first evaluation of thermodynamic data for the alloy phases. At about the same time, Wagner published a book on the same topic [3]. After 1945, systematic thermodynamic studies were undertaken in various centres all over the world. It should be mentioned that in 1972 an important symposium on ''Thermodynamics of Alloys'' was held in Münster, Germany, [4] when an informal division into those centres dealing with calculations of phase equilibria, modelling, and/or first-principle input, and the others tending more towards experimental measurements was made to some extent. This was followed in 1973 by detailed evaluations for all the metallic elements and binary alloy systems performed by Hultgren et al. [5,6] used until today as general references.

In turn, studies on phase equilibria were initiated in the 19th century. However, in practice, there was no systematic and basic information on phase diagrams published until the first edition of Hansen's book [7]. This gap was finally covered by later editions of Hansen and Anderko [8], and subsequent supplements [9,10]. These monographies contained, however, only the information about phase boundaries accompanied with some crystal structure data.

Both groups working on thermodynamic properties and phase equilibria separately developed their own ways of data collection using them adroitly to enlarge required experimental information. While traditional metallographic methods, X-ray and later neutron diffraction, differential thermal analysis as well as other physical methods were used to investigate phase equilibria, a number of methods was developed to supply thermochemical data for phases being the building elements of multicomponent systems. These experimental methods we will discuss in detail. The main aim of this paper is to demonstrate how different experimental techniques can be coupled to derive proper information necessary to establish phase equilibria. We have selected some examples from the experience accumulated over the years in our laboratories in Kraków. It should be mentioned, however, that it would not be possible to gain this experience without the help of and friendly co-operation with a number of research laboratories like NTH in Trondheim, Max-Planck Institute in Stuttgart, Centre de Thermodynamique et Microcalorimetrie du CNRS in Marseilles, University of Toronto, Iowa State University in Ames, University of Wisconsin-Madison, the University of Chicago and ASM International in USA.

It seems that the first person who suggested the mutual interconnection between the shape of the phase diagram and thermodynamic properties was Van Laar [11] in 1935. However, the real calculations of phase equilibria started after World War II with the work of Hillert [12], and later Kaufman and Bernstein [13], who introduced computers to common use.

Since then, there has been a need to combine thermodynamic data with existing information on phase equilibria to produce critically evaluated phase diagrams also for industrial purposes. The program was undertaken in 1978 by the National Bureau of Standards and the American Society for Metals resulting in new editions of Binary [14] and Ternary [15] Alloy Phase Diagrams. This research activity led to the creation of Calphad group, Journal of Phase Equilibria and initiated regular ''Thermodynamics of Alloys'' conferences. Though the real history of the phase diagram determination is more complicated, the point is that the calculations showed one very interesting and important feature of available experimental data. It would not be possible to derive the complete phase diagram even for binary system if the data used for calculation were taken from only one experimental source. There are also visible analysing examples discussed in this paper.

2. Characterisation of the experimental methods used in thermodynamic investigations

In general, there are four experimental methods, namely, calorimetry, vapour pressure, emf and phase equilibration, one can use these to derive thermodynamic functions, which describe properties of respective phases from which the whole system is composed. Those readers who would like to get some more information concerning experimental details should refer to the following publications [16–19].

2.1. Calorimetry.

Calorimetry provides the way of the determination of the heat of formation, heat capacity, heat of transformation, heat of mixing, etc. by means of a suitable device since it enables a direct measurement of the heat effects. Depending on the construction the measured heat can be stored in the calorimetric vessel and /or exchanged with the surrounding shield. Due to this fact calorimetric measurements consist in general of the measurements of temperature changes. These changes are related to the enthalpy changes, which occur due to the change of state of the investigated system. The initial and final state of the observed process must be defined precisely, which often requires an exact analysis of the reaction products. Calorimetric measurements are frequently carried out as relative measurements, i.e. they require calibration of the system with a known quantity of heat.

It is impossible to describe all calorimeters since many of them were designed to solve particular thermochemical problems. Usually, application of each type is restricted to a certain range of temperatures. In high temperature calorimetry the errors resulting from chemical interactions are more serious than the physical errors. Chemical reactions between the specimen and the container, reactions between impurities and the component substance, reactions of vapours with the insulation, are all factors affecting accuracy of the measurements. Since temperature is a parameter measured during the experiments it can be used to classify calorimeters in the following way:

- isothermal calorimeters; $T_{\text{calorimeter}}$ is equal to $T_{\text{surroundings}}$ and is constant, heat produced varies with time,
- adiabatic calorimeter; $T_{\text{calorimeter}}$ is equal to $T_{\text{surroundings}}$ and changes with the variation of heat produced,
- heat flux calorimeter; a difference $T_{\text{calorimeter}} - T_{\text{surroundings}}$ is constant,
- isoperibol calorimeter; $T_{\text{surroundings}}$ is constant while $T_{\text{calorimeter}}$ changes and is measured during reaction time.

The choice of the type of the calorimeter may depend on the type of reaction to be studied. The first distinction is between highly exothermic reaction (i.e. spontaneous) on one hand and slow reaction (e.g. dissolution) on the other. Another choice may depend on whether the system is reacting or non-reacting (heat capacity measurements). In general, calorimetry, which is a very convenient method in solving many thermochemical problems, provides very precisely the leading terms in Gibbs energies of alloy formation i.e. enthalpy changes.

2.2. Vapour pressure measurements

The weakness of the calorimetric method consists in the fact that a number of calorimetric measurements must be combined (those of the standard heat of formation, heat capacity, heat of transformations, etc.) in order to obtain the Gibbs energy changes expression for a given system. Therefore, it is sometimes more convenient to obtain standard Gibbs energy change at constant temperature from the equilibrium constant which in the simplest case of condensed state–gaseous phase equilibrium reduced to the saturation vapour pressure. Thus, from the equilibrium vapour pressure measurements standard free energy change as well as activities of components in the solution can be obtained.

In general, vapour pressure measurements can be divided into two groups:

2.2.1. Static measurements

These measurements yield the saturation total vapour pressure in the range 10^{-2} to 1 bar. A significant transfer of the material should not take place in the system. Various types of manometers are used to monitor the pressure directly. Quartz spiral manometer or Bourdon manometer allows to measure the pressure in the range from about 10^{-3} to more than 0.3 bar, at relatively high temperatures. However, it should be remembered that difficulties increase with the temperature of measurement. This method can be modified by a sealed system with well-defined volume and using optical emission or adsorption as a measure of the pressure, however, such systems need calibration.

Static method, so far described, measures pressure at constant temperature and sample composition. The operation mode can be reversed. One can determine the composition of the sample under the condition of constant pressure and temperature. This modification

is called the isopiestic technique and its successful operation requires the establishment of the equilibrium partial pressure between specimen at high temperature and pure volatile component of the specimen held at the low temperature end of a sealed vessel. Mass change of the sample or chemical analysis can be used to find equilibrium composition.

2.2.2. Dynamic measurements

These methods operate at the pressure below 10^{-3} bar. They can be divided into two groups:

- the transportation methods, and
- the effusion methods.

In the transportation method a volatile component of the alloy is carried by a steady, controlled stream of an inert gas, which passes the system under investigation at constant temperature. The vapour is condensed and the deposit is collected. Since the partial pressure is proportional to the number of moles carried by the stream, the weight change of the sample is related to the partial pressure in the gas. The flow rate is an important parameter, which decides about the saturation of the gas phase. Experiments should be carried at different flow rates to check if the real equilibrium between the sample and the gas phase is achieved.

In turn, effusion methods (Knudsen or Langmuir) determine the partial pressure by its rate of evaporation. In modern experimental arrangements the weight loss of the sample is monitored by a microbalance with sensitivity of the order of 1 μg. Potentially, the most powerful method is the effusion technique combined with mass spectrometry, which identifies and gives the partial pressure of all species present in the gas phase as a function of temperature. The other advantage of this method is that temperature of measurements can be really high and not achievable by other methods. This method can also be applied in the case when the use of an emf cell is not possible due to a close position of the alloy components in the electrochemical series. This is, for example, the case of the Cd–Ga alloys discussed later in this chapter.

It can be noticed that there is a gap in the range of pressure 10^{-2}–10^{-3} bar, which is covered by neither method. It seems the transpiration technique based on the vaporisation of the substance through the capillary tube into the condenser, can fill this gap.

2.3. Electrochemical methods

This method may be considered as the most accurate as far as the determination of the activity (partial Gibbs energy) is concerned. The disadvantage (contrary to the vapour pressure method) is that even with the application of solid electrolytes it cannot reach such high temperature of measurement as mass spectrometry.

In an electrochemical cell the amount of non-volume work necessary to transfer one mole of a chosen element of the valency n from its pure state into the solution is related to the transfer of a charge $n{\cdot}F$:

$$\Delta G = -n \cdot F \cdot E, \tag{1}$$

where E is an electromotive force produced by the cell. If the electrolyte in the cell conducts only the migrating ions, then electrons must move through an external circuit. This flow can be stopped with the high resistance (this is assured by proper measuring device) and in such a case the open-circuit potential can be measured, which corresponds to the state of thermodynamic equilibrium. It is clear from this short description that the main problem of successful cell operation consists in:

- finding a suitable electrolyte;
- proper identification of the single reversible process at each electrode.

Two general classes of cells may be employed during thermodynamic investigations.

Chemical cells in which the emf is produced due to chemical reaction occurring within the cell.

Concentration cells in which emf is generated due to free energy decrease resulting from the transfer of the same element from one electrode to the other through an electrolyte containing this element.

These cells can be assembled with the electrolytes conducting cations or anions. In general, electrolytes can be solid or liquid. While liquid electrolytes in high temperature applications are mainly halides, solid phases with ionic conductivity mostly used in thermodynamic measurements are zirconia based oxygen conductors, sodium conducting β-alumina and fluorine conductor CaF_2.

Cells of the type 1 and 2 can be designed with or without transference. Several requirements must be fulfilled to achieve reversible cell performance:

- lack of spontaneous charge transfer between electrodes. No electronic conductivity in the electrolyte, proper high resistance measuring device, no conduction at high temperature in materials used for the cell construction help to reach this requirement;
- no exchange reaction between electrolyte and the alloy components as well as with the gas phase and electric leads help to keep electrodes in the state of equilibrium;
- elimination of axial and radial thermal gradients in the cell which may result in concentration gradients. These gradients can be eliminated by proper cell construction;
- valence of the conducting element in the electrolyte should be well defined and constant in the range of temperatures in which the cell operates. If the element can exist in more than one valence state (e.g. Ga^{+1}–Ga^{+3}), then n in $-n{\cdot}F{\cdot}E$ formula is not defined and it is not clear which reaction may take place at the electrode. Sometimes, addition of the another salt to the electrolyte can control this process.

Finally, let us see how partial functions are usually derived from emf's. The results of our measurements yield a set of pairs E_i and T_i for fixed composition. In most cases we fit these data with the linear formula:

$$E = a + b \cdot T. \tag{2}$$

One can see immediately that due to the relationship:

$$\begin{aligned}\Delta G_i &= RT \cdot \ln a_i = \Delta H_i - T \cdot \Delta S_i \\ &= -n \cdot F \cdot (a + b \cdot T)\end{aligned} \tag{3}$$

not only activity a_i but also partial enthalpy and partial entropy of the alloy component can be determined directly from a and b parameters as:

$$\Delta H_i = -a \cdot n \cdot F, \tag{4}$$

$$\Delta S_i = b \cdot n \cdot F. \tag{5}$$

Both functions, however, depend on the accuracy of the determination of a and b parameters. The bigger the error in the determination of parameters of linear Eq. (2) the bigger the uncertainty of determined partial functions. However, if at this stage of investigations emf measurements can be coupled with calorimetric data, one can derive very accurately not only $\Delta G_i(X_i)$ but also $\Delta S_i(X_i)$ dependencies. Concentration dependence of partial functions may deliver interesting information about the tendency toward either ordering or segregation process in the single phase.

2.4. Phase equilibration

Activity (or partial Gibbs energy) in the alloy can also be derived from the investigations of the equilibrium between alloy and the gaseous and condensed phase (e.g. carbide, oxide, sulphide, etc.) if the latter contains the element present in the solution. This technique in principle is based on the transportation method, while the gaseous phase may consist of two or more gaseous components. Most common gas mixtures used in practice are those with:

- H_2/CH_4; fixed carbon potential;
- H_2/NH_3; fixed nitrogen potential;
- H_2/H_2O and CO/CO_2; fixed oxygen potential;
- H_2/H_2S; fixed sulphur potential;
- H_2/HCl; fixed chlorine potential.

Another possibility to obtain activity values is to investigate the phase equilibrium between metallic and non-metallic phases. This procedure is in fact reduced to the investigations of the equilibrium constant of the exchange reaction between components of the metallic and other condensed phase (e.g. oxide, silicate, chloride, etc.). Activity of one component must be known as a function of the composition in one phase at constant temperature. This method relies heavily on the accuracy of chemical analysis of phases involved in chemical equilibrium.

3. Use of experimental methods for phase equilibria determination

Let us start our considerations from the Cd–Ga system, which we can take as an example. At first sight (Fig. 1) it is a simple binary system with a small miscibility gap [20]. It seems that the regular solution model with one parameter should be sufficient for the description of the liquid solution to calculate this system. There are experimental vapour pressure measurements of Predel [21], which provided composition dependence of the activities in this system. However, if these activities are accepted, there is no way to reproduce the phase diagram exactly. What is wrong?

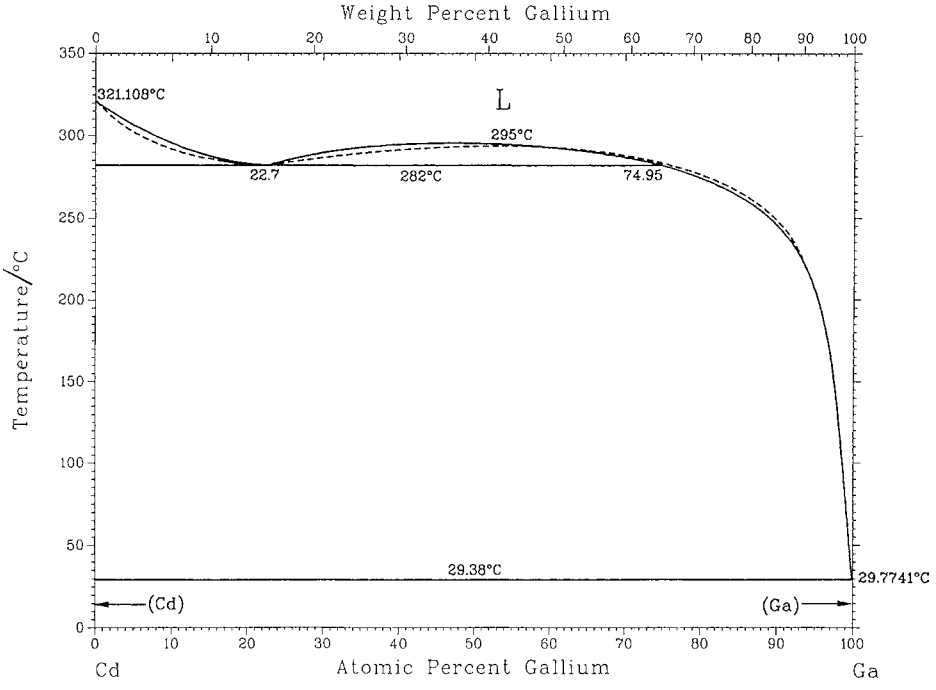

Fig. 1. Phase diagram of the Cd–Ga system [20].

The unexpected feature of these apparently simple solutions was revealed by ΔC_p measurements of liquid alloys by Moser and Fecht [22]. In Fig. 2, ΔC_p is shown as a function of gallium composition at different temperatures. It is obvious that there is a deviation from Kopp–Neumann rule and the heat of mixing must be a function of temperature in this system. Indeed, results of calorimetric measurements of Moser et al. [23] shown in Fig. 3 demonstrate that the heat of mixing of Cd–Ga liquid alloys does depend on temperature. If now this temperature dependence is included into the description of the thermodynamic properties of liquid solutions, the Cd–Ga phase diagram is exactly calculated (dotted line in Fig. 1).

The question arises: is there a way to explain this unexpected temperature dependence of the heat effect? Fortunately, in this particular case, there is. Using X-ray diffraction technique Hermann et al. [24] determined the so-called concentration–concentration fluctuation structure factor, $S_{CC}(0)$, which is shown in Fig. 4(b). This parameter defined by Bhatia and Thornton [25] has the form:

$$S_{CC}(0) = (1 - X_i) \cdot [(\mathrm{d}\ln a_i / \mathrm{d}X_i)_{T,p}]^{-1}. \qquad (6)$$

Eq. (6) allows $S_{CC}(0)$ to be calculated if the activity of one component is known as a function of temperature and composition of the alloy (in our case Cd–Ga).

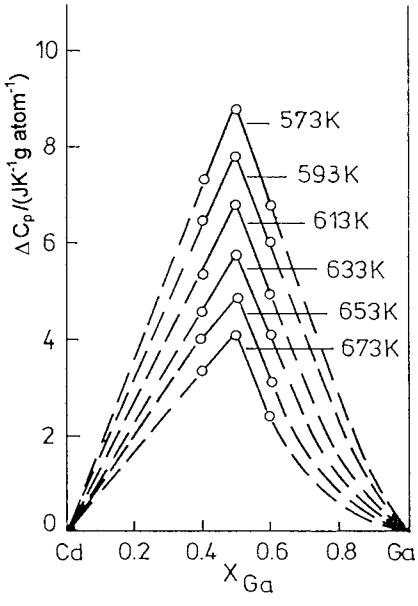

Fig. 2. Heat capacity difference in liquid Cd–Ga alloys [22].

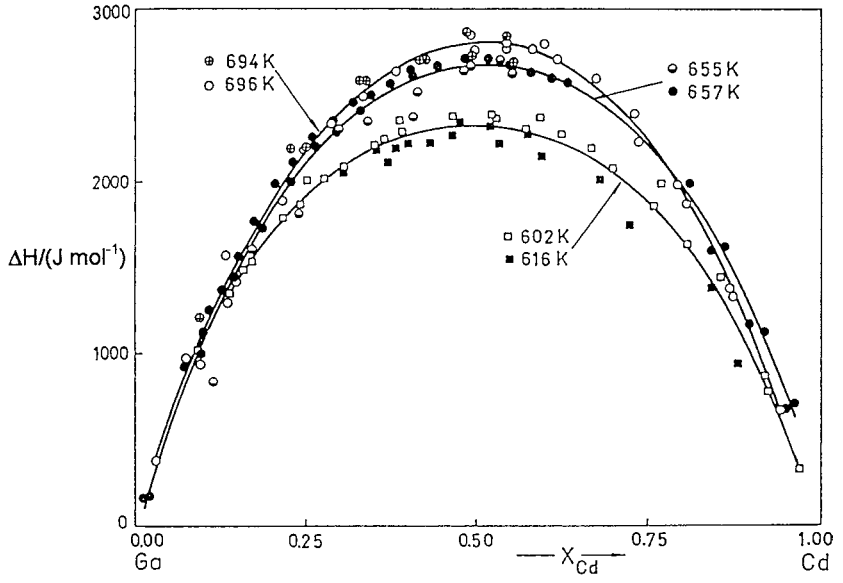

Fig. 3. Heat of mixing in liquid Cd–Ga alloys [23].

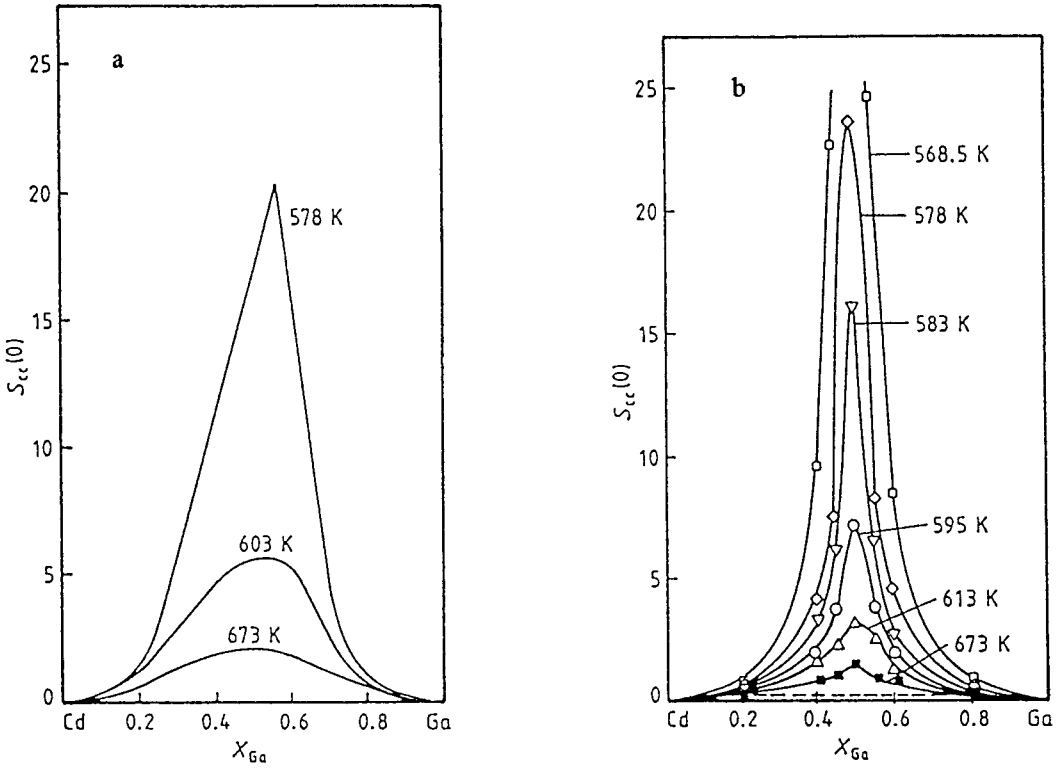

Fig. 4. (a) B–T partial structure factor calculated from Ref. [26]; (b) B–T partial structure factor from X-ray diffraction studies [24].

Calculations [26] showed full analogy between measured and predicted $S_{CC}(0)$ behaviour in the liquid Cd–Ga solution (Fig. 4(a)). The ideal solution yields $S_{CC}(0)=X_{Cd}\cdot X_{Ga}$ (atoms are distributed at random). The structure factor exceeding this value (Fig. 4(b)) shows that like-atom pairs are preferred. Thus, the information gathered from different experimental sources gave not only good description of the phase diagram, but also explained the origin of the solution's behaviour attributing the temperature dependence to the clustering of like-atoms.

Now, let us turn our attention to another powerful experimental technique, which stems from electrochemistry, and see how emf measurements can be used to verify phase equilibria. The emf measurements can themselves verify parts of phase diagrams if emf's are determined as a function of temperature and alloy composition. Fig. 5 illustrates the Mg–Li phase diagram [27] with points corresponding to temperature and composition of emf measurements carried out with the cells of the type:

$$\mathrm{Li}\,\|\mathrm{Li}^{+}\|\,\mathrm{Li}_x\mathrm{Mg}_{1-x}(\text{solid or liquid}). \qquad (7)$$

If now the results are plotted as emf vs. X_{Li} at constant temperature (Fig. 6), the phase boundaries can be derived from this plot. This study by Gąsior et al. [28] helped to verify high temperature phase equilibria in the Mg–Li system. However, emf method

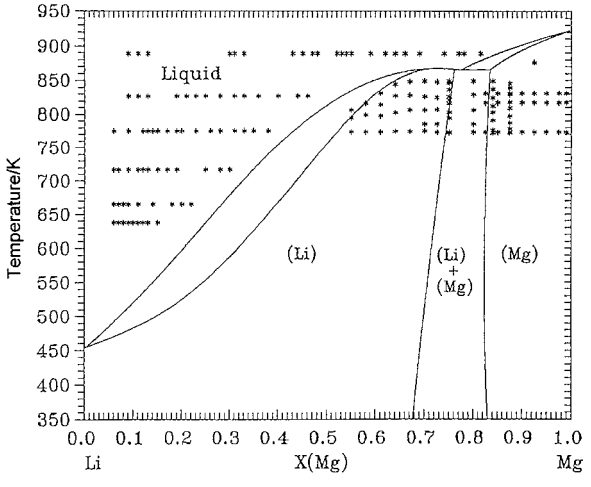

Fig. 5. Concentrations of investigated alloys in the Li–Mg system [28] by the emf method (*) with phase boundaries from Saunders [27].

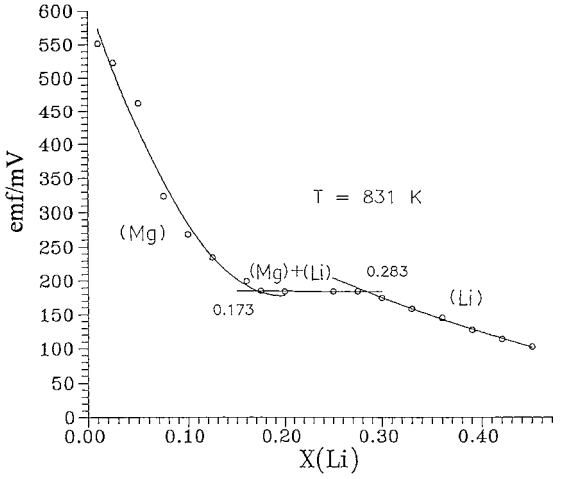

Fig. 6. An example of the determination of phase boundaries at (Li) ‖[(Mg)+(Li)] and (Mg)‖ [(Mg)+(Li)] in the solid phase of the Li–Mg system from emf studies [28].

cannot give a right answer in each case. In Fig. 7 the results of emf measurements on Mg–Sn system are shown as a function of temperature for fixed alloy composition [29]. Again, liquidus boundary can be determined directly from emf measurements. However, the Mg–Sn system has an intermetallic compound in the solid state, and one may expect strong interaction of unlike atoms in the solution. In this case negative deviation from Raoult's law and temperature dependence of the heat of mixing is expected. Indeed, integral heat of mixing shown in Fig. 8 reveals this kind of dependence [30]. In such a case, however, emf vs. temperature plot should be non-linear, which does not occur (Fig. 7). The best fit is by a straight line. In Ref. [29] the analysis of the standard deviations of the relation of emf vs. T has proved that experimental errors are higher than an expected curvilinear dependence of emf recalculated from Sommer et al.'s [30] temperature dependence of the integral heat of mixing (maximum values are of the order of 2 mV). In such a case one may look at the results of other methods to confirm the temperature dependence. Results of such measurements together with the integral heat of mixing are gathered in Fig. 8 for Mg–Sn system [31]. Their behaviour is typical of systems, in which negative deviation from Raoult's law is expected, though emf's alone do not indicate this.

The determination of physical properties may sometimes result in the phase boundary identification.

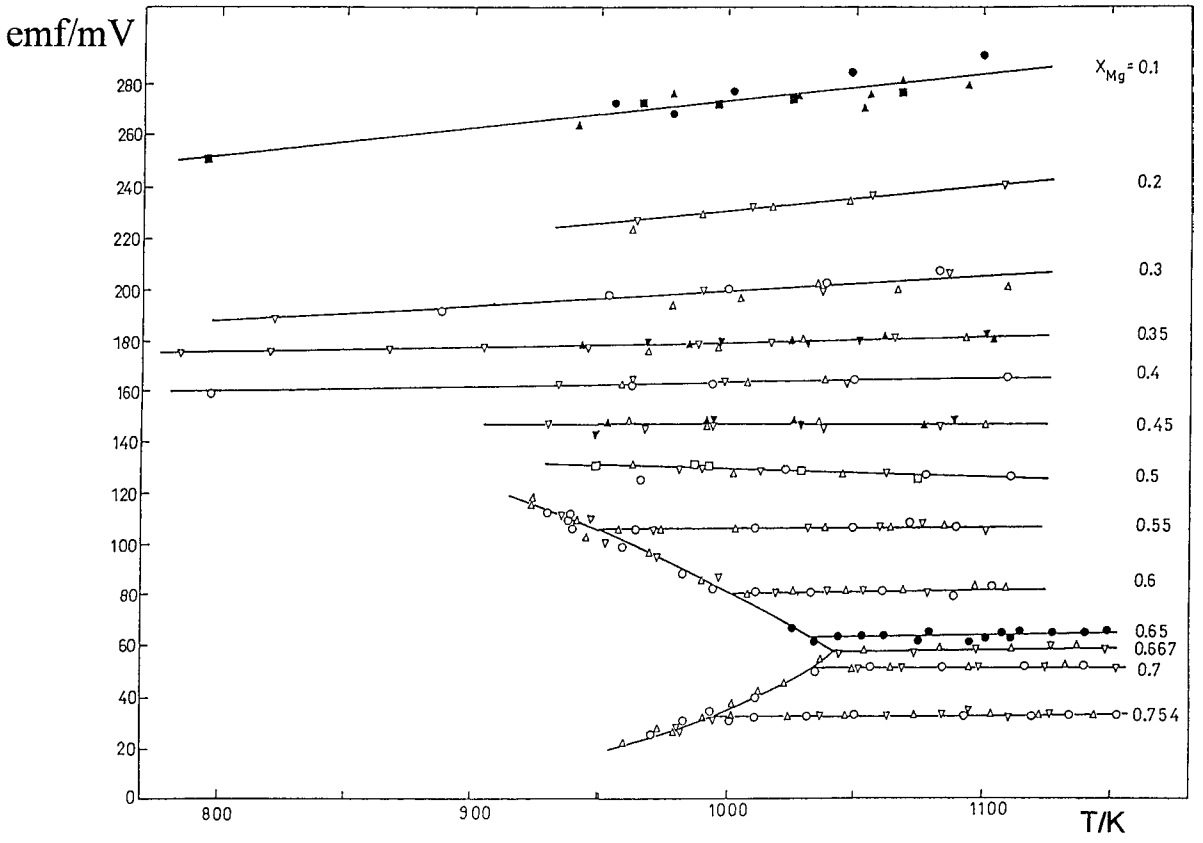

Fig. 7. Temperature dependence of the emf of liquid Mg–Sn alloys relative to the liquid magnesium reference electrode [29], ■ ● ▲ ▼ – weighted-in alloys, ○ □ Δ ∇ – coulometric titrated alloys.

As an example, investigations of the resistivity of liquid In–Ga alloys can be given. Using DC four-probe method we determined resistivities of the liquid In, Ga and their alloys [32]. The results of our measurements showing solid–liquid transitions for a given sample composition were imposed on the In–Ga phase diagram (Fig. 9), and reproduced the phase equilibria [8] exactly. The method seems to be sensitive enough to detect even small effects accompanied with phase changes.

Electrochemical measurements alone can be refined even further. Since experiments carried out for a number of samples with different compositions are both time consuming and expensive, one may try to change the composition of the alloy by passing controlled amount of electricity through the cell. Since the charge passed is connected via Faraday's law with the number of moles transferred, one may change the composition of the sample starting from its pure state. The results of the application of this technique, called coulometric titration, to Li–Sn system are shown in Fig. 10. In this figure the partial Gibbs energies of lithium measured at different temperatures in liquid alloys [33] are compared with literature data. Since the composition of the samples was changed by titration it demonstrates the reliability of results and of the method itself. In Fig. 11 results of similar measurements carried out on solid alloys are shown. It is seen that changing composition by titration at constant temperature allows to identify phase boundary as well as homogeneity range of phases.

From these considerations one may draw the following conclusion:

- there is no better way to yield enthalpy data than calorimetry;

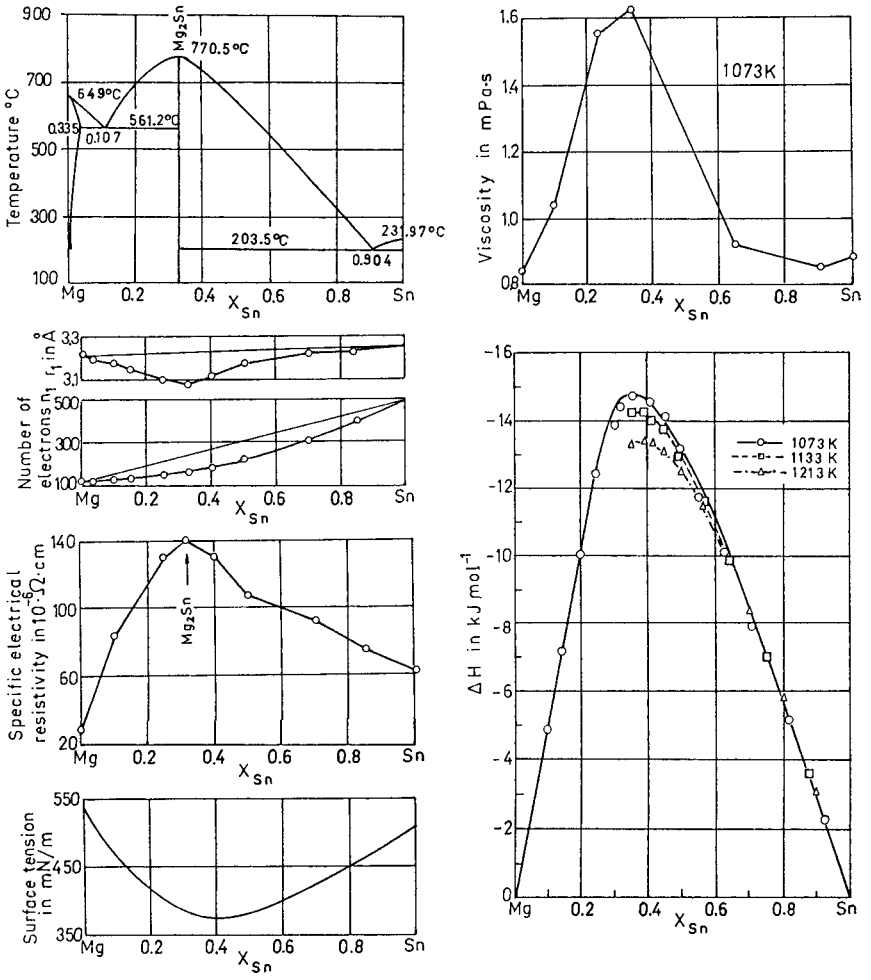

Fig. 8. Comparison of the physical, structural and thermodynamic properties of liquid Mg–Sn alloys [31]. The following information plotted vs. X_{sn} is given starting from the top: phase diagram, atom radius of the first coordination shell and electron distribution curve in the first coordination shell, specific electrical resistivity, surface tension, viscosity and integral molar enthalpy [30].

- the most accurate activity measurements in the solution stem from emf.

Thus, to provide an exact description of the thermodynamic properties of solutions, calorimetry and electrochemical methods should be used together. This description should be satisfactory for the phase diagram calculation. As a successful demonstration of this point of view Al–Mg phase diagram can be taken as an example.

To calculate the phase diagram of the Al–Mg system, thermodynamic description of all existing phases has to be done. While the data for solid alloys were accepted from literature, activities for liquid Al–Mg alloys have been recently determined by means of galvanic cells with liquid and solid CaF_2 electrolytes, and from vapour pressure measurements [41]. In addition, vapour pressure measurements made it possible to determine the liquidus temperature for certain alloys on both the Mg-rich and Al-rich sides of the concentration (these points are included in Fig. 12 showing the phase diagram). In the same paper we have presented our calorimetric measurements of the integral enthalpy. As a result of these experiments and

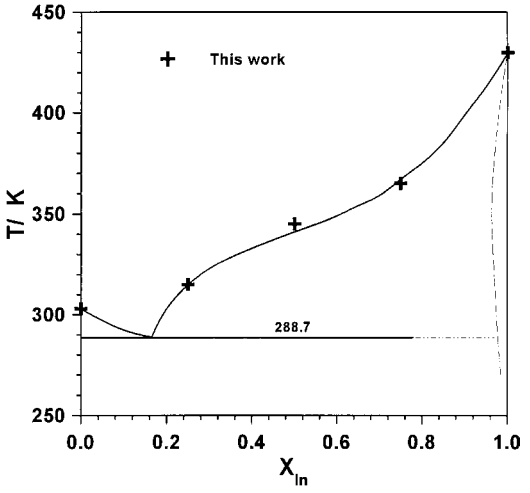

Fig. 9. Ga–In phase diagram with measured liquidus points [32]. - - - after Hansen [8].

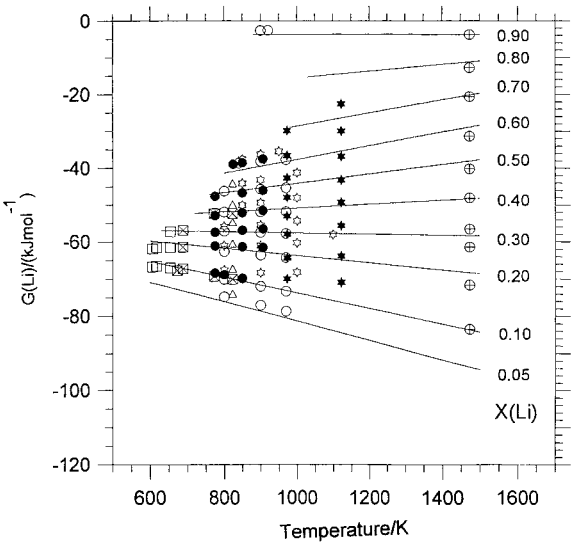

Fig. 10. Partial Gibbs energy of Li in liquid Li–Sn alloys from Ref. [33] – ○, compared with data of Fischer and Johnson [34] – ⊕, Moser et al. [35] – ●, Morachevskii et al. [36] – Δ, Baradel et al. [37] – ✸, Foster et al. [38] – ☆, Wen and Huggins [39] – ☒ and Barsoum and Tuller [40] – □.

of the optimisation of all available data both for thermodynamics and that for the phase equilibria, existing phases of the Al–Mg system were described by various models and used for phase diagram calculations by means of Lukas program [42]. The phase diagram calculated from thermodynamic data [43] is presented in Fig. 12 and compared with previous results based mainly on thermal analysis. The calculated phase diagram [43] is in good agreement with previous similar calculations [44,45] and with the data from thermal analysis.

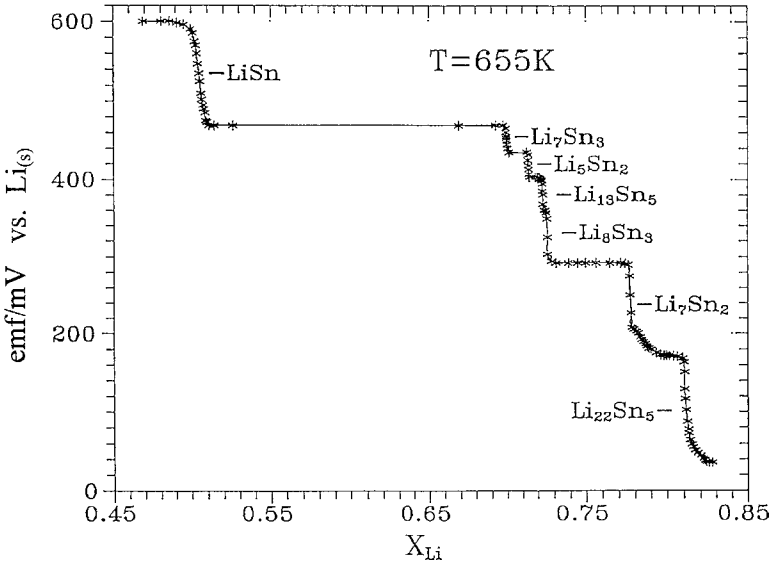

Fig. 11. Coulometric titration curve for the Li–Sn system at 665 K [33].

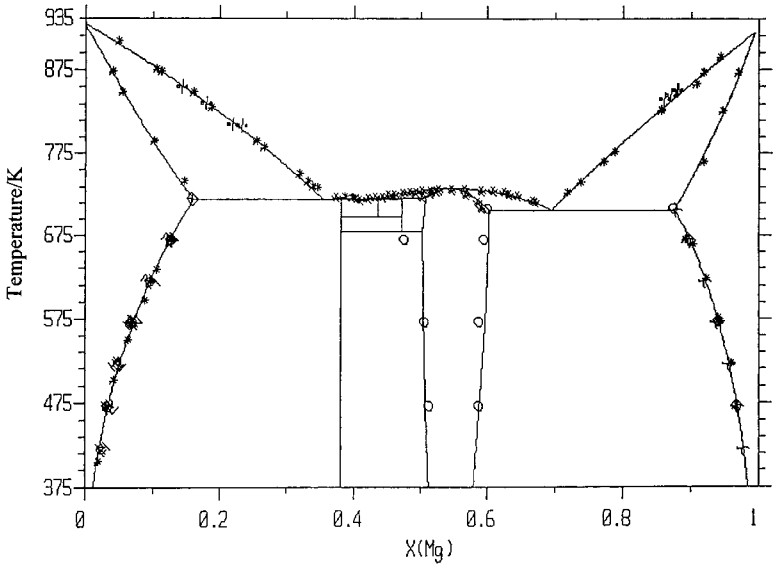

Fig. 12. The Al–Mg phase diagram. Moser et al. [41] – □/▽, Schürmann and Voss [46] – ○, Eickhoff and Vosskuhler [47] – ⊥, Schürmann and Geissler [48] – ✳, Siebel and Vosskuhler [52] – \, Raynor [53] – ◎, Saldau and Sergeev [54] – ≈, Schmid and Siebel [51] – ⊥, Dix and Keller [49,50] – Z.

4. Support from phase equilibria investigations

So far we have looked at the phase diagram as at the graphical representation of the thermodynamic properties of phases from which the whole diagram can be built. This approach requires detailed knowledge of thermodynamic properties of these phases. However, once we try to answer the question how existing data bases can be improved to get successful evaluation of phase equilibria, one may come to the conclusion that thermodynamic properties alone are not enough. It is time to demonstrate that the knowledge of phase equilibria is often needed to support thermodynamic measurements. We demonstrate this point considering alloys with arsenic. We chose arsenic because Poland is a big copper producer and most problems connected with industrial processes stem from arsenic presence in the ore. So, we were interested in the copper–arsenic system. However, after relatively short time we discovered that properties of liquid solutions do not correspond well to Gibbs energy of formation of Cu_3As if data from thermochemical tables of Barin et al. [55] are taken. In the literature we found two recent evaluations of Cu–As phase diagram: one by Teppo and Taskinen [56] and another by Sundman et al. [57]. Both works end up with conclusions that there must be something wrong with $\Delta G^0_{f,Cu_3As}$. We traced the origin of the thermochemical data in the literature and found out that the possible reason for that is an old value of the standard heat of formation of Cu_3As of Savelsberg [58], which must be apparently wrong. Now it was time to use calorimetry in order to clarify this situation. Using a Calvet-type calorimeter calibrated for quartz, and sealed quartz ampoules with alloy samples [59], we obtained the heat of mixing of liquid alloys and the standard heat of formation. All these data are shown in Fig. 17. This result is now compatible with the heat of formation of similar copper phases (Table 1).

The procedure of deriving thermochemical data from calorimetric experiments can be even better demonstrated on Ge–As system. In Fig. 13 this system is shown in two versions: (a) upper diagram, given in Alloy Phase Diagrams [14], and (b) as suggested by Ansara and Dutartre [60]. One can notice a significant difference in the As-rich part of the diagrams. More thermodynamic data are needed to verify the correct version. We used similar calorimetric experiments to obtain standard heat of formation and the heat of mixing in the liquid state between arsenic and silicon,

Table 1
Value of ΔH_f^0 (298 K), heat content and heat of mixing, in (kJ/g atom)

System	T (K) (Exptl.)	Heat content (*T*-298 K)	ΔH_r^0 (298 K)		ΔH_{l-1}^M	
			Exptl.	Predicted	Exptl.	Predicted
$Cu_{0.75}As_{0.25}$	1113	32.46±1.42	−3.5±0.9	−18	−9.6±0.6	−8.3
$Cu_{0.75}As_{0.25}$			−26.8 (Savelsberg)			
$Cu_{0.75}P_{0.25}$			−8.7±0.9 (Kleppa's laboratory)			
$Cu_{0.75}Ge_{0.25}$			−4.1±0.6 (Kleppa's laboratory)			
$Cu_{0.75}Sb_{0.25}$			0.6 (Kleppa's laboratory)			

germanium and tin [61]. Results of our experiments, gathered in Table 2, can be used to derive Gibbs energy of formation of solid GeAs and $GeAs_2$ solid phases. The procedure is as follows:

- at first, one can calculate Gibbs energy of formation of liquid phases of these compositions at their melting points. Activities at phase compositions can be derived from sub-regular solution model with parameters obtained from our heat of mixing data and the Ge-rich side of the phase diagram;
- next, knowing the Gibbs energy of pure, liquid Ge and As at these temperatures, and the reaction of the phase formation:

$$As_{(1)} + Ge_{(1)} = GeAs_{(1)}, \quad (8)$$

$$2As_{(1)} + Ge_{(1)} = GeAs_{2\,(1)}, \quad (9)$$

  chemical potential of the pure liquid compound can be obtained from $\Delta G_{f,T}^0$ values;
- finally, once Gibbs energy of the phase at its melting temperature is known, one can calculate it back to T=298 K using heats of fusion and heat capacities measured by Blachnik and Schneider [62]. Having our standard heat of formation it is easy now to derive standard entropy S_{298}^0 for both phases.

Results of these calculations are shown in Table 3. When the standard entropy is then plotted as a function of arsenic mole fraction, almost linear dependence is obtained (Fig. 14). When the calculated Gibbs energy of formations of GeAs and $GeAs_2$ (Fig. 15) was used it was possible to calculate with ThermoCalc software the whole binary diagram (Fig. 16), but only under the assumption of ideal solid solutions. To calculate the binary diagram exactly, still more information is needed about the solid solution at the As-rich side. Either the solubility of Ge in arsenic must be reliably known (we think that the solubility range shown in Fig. 13 is wrong) or we must know the activities of components in Ge–As solid solution (which in turn is very difficult to measure). At present, we know none of them. It is an example when at certain point the knowledge of phase equilibria must be used to support the process of calculations. This point we would like to discuss a little further. Two more examples may be given from the field of ceramic systems.

Table 2
Value of ΔH_f^0 (298 K), heat content and heat of mixing, in (kJ/g atom)

System	T (K) (Exptl.)	Heat content (*T*-298 K)	ΔH_f^0 (298 K)		ΔH_{l-1}^M	
			Exptl.	Predicted	Exptl.	Predicted
$As_{0.5}Si_{0.5}$	1123.00	20.1±1.1	−5.4±1.2	−114.00		
$As_{0.67}Si_{0.33}$	1123.00	24.1±1.9	−3.7±2.3	−89.00		
$As_{0.5}Ge_{0.5}$	1058.00	52.6±2.1	−5.5±2.6	−121.00	−2.8±1.5	−65.00
$As_{0.67}Ge_{0.33}$	1058.00	51.6±2.6	−5.8±3.2	−96.00	−2.6±1.9	−57.00
$As_{0.5}Sn_{0.5}$	987.00	41.0±2.4	−9.5±3.2	−150.00	−2.8±2.2	−74.00
$As_{0.3}Sn_{0.7}$	987.00				−3.3±1.1	
$As_{0.7}Sn_{0.3}$	987.00				−2.5±0.1	

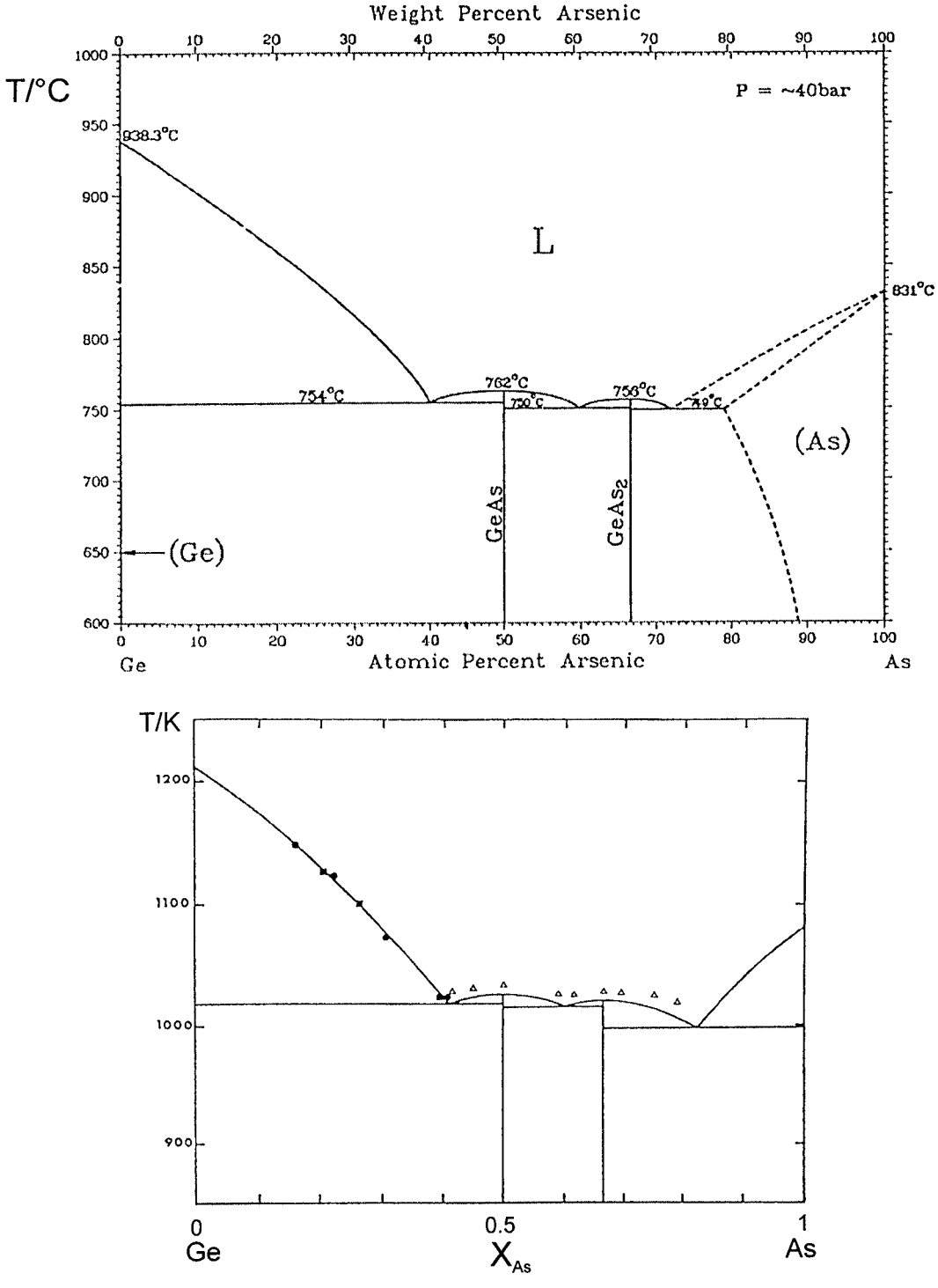

Fig. 13. Ge–As phase diagram. Upper diagram: Ref. [14], lower diagram: Ref. [60].

Table 3
Thermochemical data calculated for GeAs and $GeAs_2$ phases (per mol compound)

T (K)	H^0 (kJ/mol)	S^0 (J/mol K)	G^0 (kJ/mol)	ΔG^0 (kJ/mol)
GeAs, $\Delta H^0_{298}=-11$ kJ/mol, $S^0_{298}=63.3$ J/mol K, Ge+As=GeAs				
298	−11.00	63.30	−29.86	−10.12
300	−10.92	63.51	−29.97	−10.08
400	−5.85	78.37	−37.20	−9.36
500	−0.53	89.68	−45.37	−8.75
600	4.49	99.31	−55.09	−8.88
700	9.93	107.68	−65.44	−8.81
800	15.80	115.22	−76.38	−8.51
900	21.24	121.92	−88.49	−8.56
1000	27.10	127.78	−100.68	−7.87
1025	28.77	129.45	−103.91	−7.76
1025	92.83	191.83	−103.80	−7.64
1100	99.11	197.70	−118.35	−11.84
$GeAs_2$, $\Delta H^0_{298}=-17.4$ kJ/mol, $S^0_{298}=95.2$ J/mol K, Ge+2As=$GeAs_2$				
298	−17.40	95.20	−45.77	−15.53
300	−17.27	95.60	−45.96	−15.49
400	−10.28	116.10	−56.74	−14.13
500	−2.75	132.50	−68.98	−13.01
600	4.79	146.70	−83.23	−12.67
700	13.16	158.80	−98.02	−11.66
800	21.54	170.10	−114.58	−11.18
900	30.33	180.60	−132.22	−10.57
1000	39.12	189.80	−150.70	−9.57
1021	41.22	191.90	−154.73	−9.36
1021	127.88	276.90	−154.84	−9.47
1100	140.44	288.60	−177.05	−15.21

In the CuO–BaO–lanthanide oxide systems the ⟨123⟩ phase appears, which is considered to be a high temperature superconductor. To obtain information about its thermodynamic stability one way is to use electrochemical measurements with zirconia and CaF_2 solid electrolytes. A schematic representation of the phase equilibria, shown in Fig. 17, suggests how these measurements can be conducted. If the stability of the double oxide either $Cu_2Ln_2O_5$ or $CuLn_2O_4$ is known from emf measurements, then the stability of the ⟨211⟩ – "green" phase can be obtained with the cells with CaF_2 electrolyte from CuO–⟨211⟩–$Cu_2Ln_2O_5$ ($CuLn_2O_4$) phase equilibrium. Then, using the same technique either the stability of ⟨123⟩ phase can be determined from CuO–⟨211⟩–⟨123⟩ phase equilibrium or the stability of ⟨123⟩-based solid solution can be determined from CuO–⟨211⟩–⟨336⟩ phase equilibrium. The element, which decides about the formation of ⟨123⟩-based solid solution, seems to be either Gd or Eu. Using both types of cells we decided to determine thermodynamic stabilities of all these phases.

At first, using zirconia electrolytes, the Gibbs energies of formation of $Cu_2Ln_2O_5$ for *Ln*=Yb, Tm, Er, Ho, Dy and Gd were determined [63]. Next, using these data, the Gibbs energy of formation of respective Ln_2CuBaO_5 phases was derived from our emf measurements [64]. Finally, Gibbs energy of formation of $LnBa_2Cu_3O_{7-x}$ phases for the same lanthanide elements was determined [65].

The last example appeared to be our spectacular failure. Having the stability of $Cu_2Ln_2O_5$ and Ln_2CuBaO_5 phases we wanted to determine Gibbs energy of formation of *Ln*⟨123⟩ phases. We started our measurements from Yb⟨123⟩, but using the conventional method of making these compounds from CuO, $BaCO_3$ and Yb_2O_3 we failed. After a couple of weeks of attempts we found a paper of Zhang and Osamura

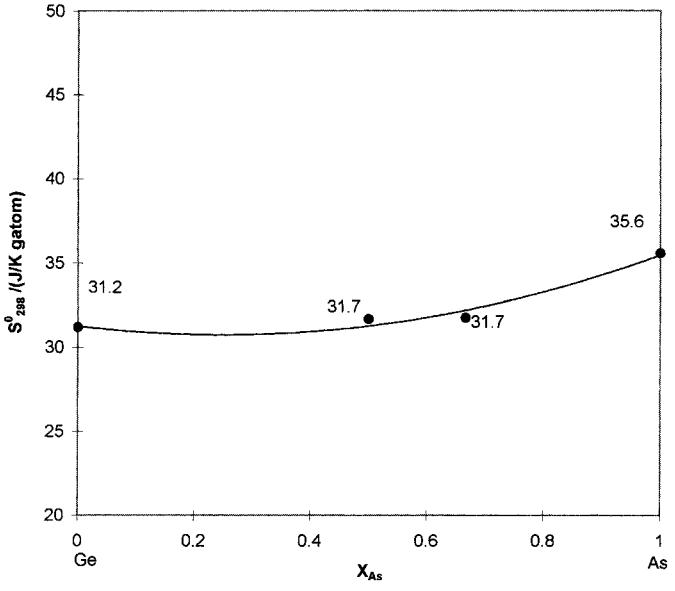

Fig. 14. Standard entropy vs. X_{As} in the Ge–As system.

[66]. The secret of Yb⟨123⟩ phase formation is shown in Fig. 18. As it happens it should be synthesised at high temperature under reduced oxygen pressure! If the synthesis is carried out as usual in air or oxygen it will decompose on cooling. When we made this compound properly and assembled the cell:

$$\text{air},\ \text{CaO} + \text{CaF}_2 \,\|\text{CaF}_2\|\, \text{Yb}\langle 123\rangle + \text{Yb}\langle 211\rangle + \text{CuO} + \text{BaF}_2,\ \text{air} \qquad (10)$$

we obtained the results as shown in Fig. 19. The cell worked reversibly for about a week and Gibbs energy of the Yb⟨123⟩ phase was determined [65]. One more

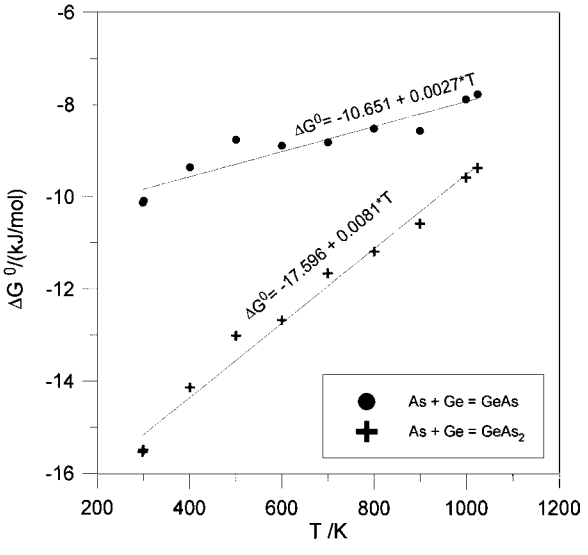

Fig. 15. Gibbs energy of formation of GeAs and $GeAs_2$ phases as a function of temperature.

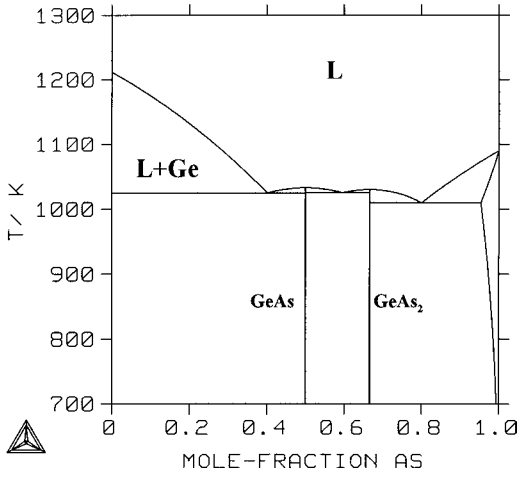

Fig. 16. Calculated Ge–As phase diagram.

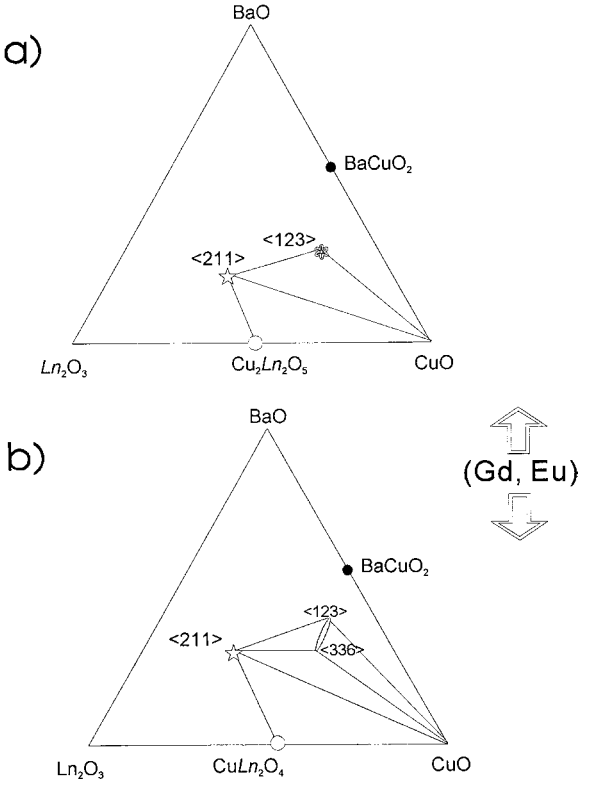

Fig. 17. Schematic diagram of phase equilibria in the CuO-rich corner of the Ln_2O_3–BaO–CuO systems.

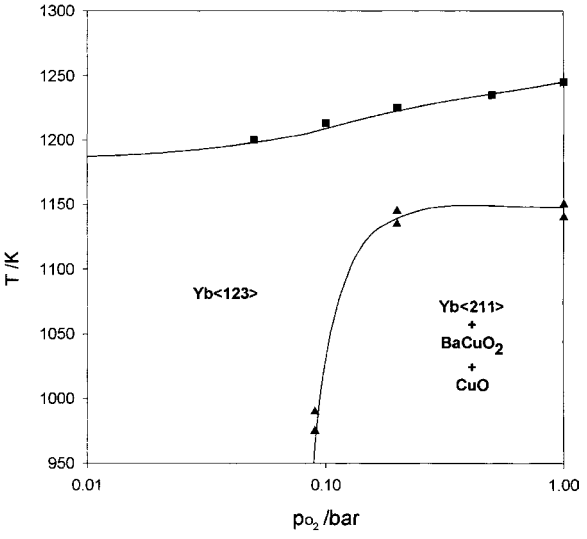

Fig. 18. Stable region of the Yb⟨123⟩ phase [66].

time, the knowledge in phase equilibria helped us to accomplish the thermodynamic measurements.

5. Conclusion

It has been shown starting from the historical background how two separate directions of research con-

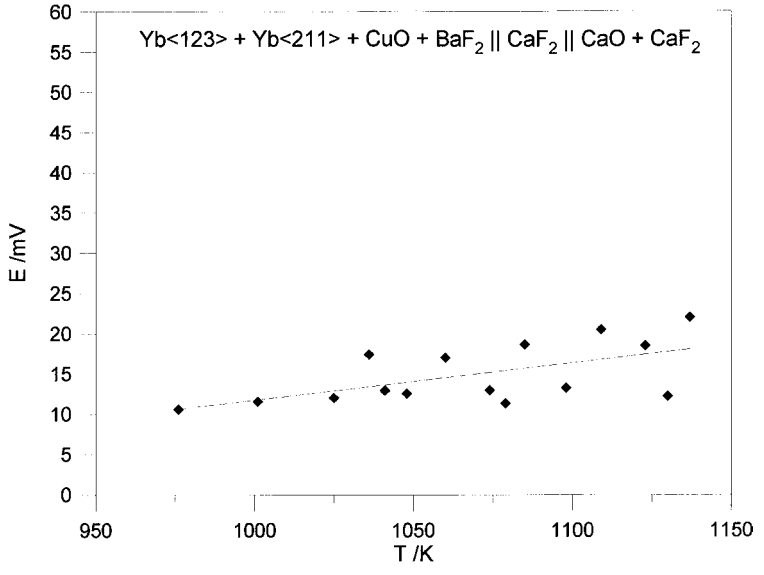

Fig. 19. Measured temperature dependence of the emf produced by the cell (10).

nected with thermodynamic experimental studies on one hand, and investigations of phase equilibria on the other, have been coupled. Also, limitations of various experimental techniques applied to thermodynamic studies have been discussed. We have shown that the time is over when results obtained from one experimental technique were considered to be satisfactory for the proper description of thermodynamic functions characterising the system.

The reliable approach to the precise division of Gibbs energy into enthalpy and entropy terms is to combine the results of either emf or vapour pressure studies with calorimetric measurements. Further development of the methods of calculations and verifications of phase equilibria is based not only on advances of theoretical modelling but also on new thermodynamic data derived from experiments. The renaissance of the experimental studies was well seen during the recent Calphad meeting in May 1997 in Orlando, FL as well as it can be observed in the increasing amount of publications in various scientific journals all over the world.

The results of experimental thermodynamic studies may verify directly the phase boundaries but nowadays the most elegant way is to use them after critical evaluation for phase diagram calculation. Due to enormous progress in computer application phase diagrams can now be reproduced with great accuracy. This was also the purpose of ASM-NBS project initiated about twenty years ago. Poland has participated in this project and as a result Polish Phase Diagram Committee was created in 1994, which is a member of Alloy Phase Diagram International Commission associated with ASM International.

References

[1] K.K. Kelley, Contribution to the Data on Thermochemical Metallurgy, Bureau of Mines Bull. (1935) 383.

[2] F. Weibke, O. Kubaschewski, Thermochemie der Legierungen, Springer, Berlin, 1943.

[3] C. Wagner, in: G. Masing (Ed.), Thermodynamik metallischer Mehrstoffsysteme, published in Handbuch der Metallphysik, vol. I, Part 2, Akademische Verlagsgesellschaft Becker and Erler, Kom.-Ges., Leipzig, 1940.

[4] Symposium, Thermodynamik der Legierungen, Münster (Westfan), 27–28 September 1972.

[5] R. Hultgren, P.D. Desai, D.T. Hawkins, M. Gleiser, K.K. Kelley, Selected Values of the Thermodynamic Properties of Binary Alloys, American Society for Metals, Metals Park, OH, 1973.

[6] R. Hultgren, P.D. Desai, D.T. Hawkins, M. Gleiser, K.K. Kelley, D.D. Wagman, Selected Values of the Thermodynamic Properties of the Elements, American Society for Metals, Metals Park, OH, 1973.

[7] M. Hansen, Der Aufbau der Zweistofflegierungen, Springer, Berlin, 1936.

[8] M. Hansen, K. Anderko, Constitution of Binary Alloys, originally published by McGraw-Hill, reprinted and available from Genium Publishing Corporation, 1145 Catalyn Street, Schenectady, New York 12303 (1958).

[9] R.P. Elliot, Constitution of Binary Alloys, First Supplement, originally published by McGraw-Hill, reprinted and available from Genium Publishing Corporation, 1145 Catalyn Street, Schenectady, New York 12303 (1965).

[10] F.A. Shunk, Constitution of Binary Alloys, Second Supplement, originally published by McGraw-Hill, reprinted and available from Genium Publishing Corporation, 1145 Catalyn Street, Schenectady, New York 12303 (1969).

[11] J.J. van Laar, Die Tthermodynamik einheitlicher Stoffe und binarer Gemische mit Anwendungen auf verschiedene physikalisch–chemische Probleme, P. Noordhoff Verlag, Groningen und Batavia (1935).

[12] M. Hillert, Calculation of Phase Equilibria, in: Phase Transformations, ASM, Metals Park, OH, 1970, p. 181.

[13] L. Kaufman, H. Bernstein, Computer Calculation of Phase Diagrams, Academic Press, New York, London, 1970.

[14] T.B. Massalski, P.R. Subramanian, H. Okamoto, L. Kacprzak, Binary Alloy Phase Diagrams, 2nd ed., vol. 1, 2 and 3, ASM International, Materials Park, OH, 1990.

[15] P. Villars, A. Prince, H. Okamoto, Handbook of Ternary Alloy Phase Diagrams, ASM International, Materials Park, OH, 1995.

[16] R. Castanet, Calorimetric methods in metallurgy, in: H. Brodowsky, H.J. Schaller (Eds.), Thermochemistry of Alloys, Kluwer Academic Publishers, 1989, pp. 145–168.

[17] K.L. Komarek, Z. Metallkd. 64 (1973) 325.

[18] K.L. Komarek, Z. Metallkd. 64 (1973) 406.

[19] C.B. Alcock, O. Kubaschewski, Metallurgical Thermochemistry, 5th ed., Pergamon Press, 1979.

[20] Z. Moser, J. Dutkiewicz, W. Gąsior, J. Salawa, Bull. Alloy Phase Diagrams 9 (1988) 691.

[21] B. Predel, Z. Metallkd. 49 (1958) 226.

[22] Z. Moser, H. Fecht, Z. Metallkd. 77 (1986) 377.

[23] Z. Moser, R. Castanet, K. Rzyman, S.L. Randzio, Z. Metallkd. 76 (1985) 596.

[24] G. Hermann, R. Bek, S. Steeb, Z. Naturforsch. 35a (1980) 930.

[25] A.B. Bhatia, D.E. Thornton, Phys. Rev. B 2 (1970) 3004.

[26] Z. Moser, W. Gąsior, N.A. Gokcen, J. Phys. F: Met. Phys. 18 (1988) 2363.

[27] N. Saunders, Calphad 14 (1990) 61.

[28] W. Gąsior, Z. Moser, W. Zakulski, G. Schwitzgebel, Met. Mat. Trans. 27A (1996) 2419.

[29] Z. Moser, W. Zakulski, Z. Panek, M. Kucharski, L. Zabdyr, Met. Trans. B 21B (1990) 707.

[30] F. Sommer, J.J. Lee, B. Predel, Z. Metallkd. 71 (1980) 818.
[31] S. Steeb, H. Entress, Z. Metallkd. 57 (1966) 803.
[32] B. Onderka, K. Fitzner, Arch. Met. 41 (1996) 283.
[33] W. Gąsior, Z. Moser, W. Zakulski, J. Non-Cryst. Solids 205 206 207 (1996) 379.
[34] A.K. Fisher, S.A. Johnson, J. Chem. Eng. Data 17 (1972) 280.
[35] Z. Moser, W. Gąsior, F. Sommer, G. Schwitzgebel, B. Predel, Met. Trans. 17B (1986) 791.
[36] A.G. Morachewskii, L.N. Gerasimenko, A.I. Demidov, O.A. Drozdova, Elektrokhimiya 8 (1972) 1622.
[37] P. Baradel, A. Vermande, I. Ansara, P. Desre, Rev. Int. Hautes Temp. Refract. 8 (1971) 201.
[38] M.S. Foster, C.E. Crouthamel, S.E. Wood, J. Phys. Chem. 70 (1966) 3042.
[39] C.J. Wen, R.A. Huggins, J. Electrochem. Soc. 128 (1981) 1181.
[40] M.W. Barsoum, H.L. Tuller, Met. Trans. 19A (1988) 637.
[41] Z. Moser, W. Zakulski, K. Rzyman, W. Gąsior, Z. Panek, I. Katayama, T. Matsuda, Y. Fuku-da, T. Iida, Z. Zajaczkowski, J. Botor, J. Phase Equil. 19 (1998) 38.
[42] H.L. Lukas, E.Th. Henig, B. Zimmermann, Calphad 1 (1977) 225.
[43] W. Zakulski, Z. Moser, Arch. Met. 43 (1998) 201.
[44] N. Saunders, Calphad 14 (1990) 145.
[45] Y. Zuo, Y.A. Chang, Calphad 17 (1993) 161.
[46] E. Schurmann, H.J. Voss, Giessereiforschung 33 (1981) 43.
[47] K. Eickhoff, H. Vosskuhler, Z. Metallkd. 44 (1953) 223.
[48] E. Schurmann, I.K. Geissler, Giessereiforschung 32 (1980) 167.
[49] E.H. Dix, F. Keller, Z. Metallkd. 21 (1929) 205.
[50] E.H. Dix, F. Keller, J. Inst. Met. 241 (1929) 488.
[51] E. Schmid, G. Siebel, Z. Metallkd. 23 (1931) 202.
[52] G. Siebel, H. Vosskuhler, Z. Metallkd. 31 (1939) 359.
[53] G.V. Raynor, Annoted Equilibrium Diagram, Series No. 5, Institute of Metals, London, 1945.
[54] P. Saldau, L.N. Sergeev, Metallurg. 67 (1934) 200.
[55] I. Barin, O. Knacke, O. Kubaschewski, Thermochemical Properties of Inorganic Substances (Supplement), Springer, Berlin, 1977.
[56] O. Teppo, P. Taskinen, Scand. J. Met. 20 (1991) 141.
[57] B. Pei, B. Bjorkman, B. Jansson, B. Sundman, Z. Metallkd. 85 (1994) 178.
[58] W. Savelsberg, Metall. Erz. 33 (1936) 379.
[59] J. Wypartowicz, K. Fitzner, O.J. Kleppa, J. Alloys Comp. 217 (1995) 1.
[60] I. Ansara, D. Dutartre, Calphad 8 (1984) 323.
[61] K. Fitzner, O.J. Kleppa, J. Alloys Comp. 238 (1996) 187.
[62] R. Blachnik, A. Schneider, J. Chem. Thermodyn. 3 (1971) 227.
[63] M. Kopyto, K. Fitzner, J. Mater. Sci. 31 (1996) 2797.
[64] M. Kopyto, K. Fitzner, J. Sol. State Chem. 134 (1997) 85.
[65] M. Kopyto, K. Fitzner, J. Sol. State Chem., 1998, in print.
[66] W. Zhang, K. Osamura, Z. Metallk. 84 (1993) 522.